Proc. of SPIE Vol. 0518, Optical Systems Engineering IV, ed. P.R. Yoder, Jr. (Oct 1984) Copyright SPIE

Balanced thermal deflection approach for beam handling in medium power optical systems

T. L. Miller and R. D. Grigg

Research and Engineering, US Apparatus Division, Eastman Kodak Company
Rochester, New York 14650

Abstract

Optical systems including those applied in the areas of optical communication and optically assisted chemistry can involve energies of the order of 0.1 to 3 watts deposited in system optical elements. These energy levels are sufficient to induce significant bending of elements due to thermal gradients and to raise average elements temperature substantially.

We have considered several forms of fused silica and ULE mirrors that control both the gradient induced bending and reduce the overall temperature rise. These mirror forms make use of high thermal conductivity materials bonded to the basic mirror and applications of conductively coupled heat sinks to reduce the effects of the thermal loads. We have found that a typical 2.5 cm diameter beam will result in surface deformations of less than 0.004 microns (peak) per deposited watt for steady-state conditions. For symmetric loading the majority of this deformation is found to be power.

Finite element models of several mirror forms have been utilized to predict the detailed deflection distribution of the thermally loaded mirrors. Nastran predicted deflections were then decomposed into Zernike polynomial representations of the surface.

By utilizing material choice as a degree of freedom in multi-element system design, we have found it possible to define beam handling systems that have very little thermally induced defocus for symmetric thermal loading. Heat rejection from the system utilizes controlled conduction to minimize structural deflections of the supporting structure. For asymmetric loading, higher order aberrations begin to appear and the control of thermally induced system wavefront error becomes more difficult. The major aberration, however, continues to be power for a significant range of beam decenter. Mounting geometry, thermal conductor configuration and bonding effects were included in the analysis. Good agreement between closed form and finite element analysis results was found for simplified check cases.

Introduction

Steady state thermal excitation of elements in an optical system can pose a problem from design analysis, system budgeting and operational standpoints if thermal loads are large enough to cause significant wavefront disturbances. When thermal loading is moderate, a system wavefront error budgeting analysis can be used to allocate a fixed portion of the overall allowable system error to these thermal effects. The allocated thermal error then needs to be matched with what is achievable with element optical-mechanical-thermal behavior. Consideration inherent in the analysis are (1) absorbed power level and power density, (2) ambient to steady state operating temperature changes in the elements, (3) operating temperature level, (4) temperature and thermal gradient control ,and (5) aberration forms for symmetric and asymmetric loading situations. The objective of this paper is to present the problem of system and component thermal control and discuss the results obtained with a passive thermal control approach that minimizes both temperature rise and temperature gradients within system components, and permits significant reduction of the net thermally generated power for a wide range of system configurations.

Error allocation process

Wavefront (or related parameter) error budgeting and allocation for most conventional systems normally begins with a system performance based determination of the overall error level that can be tolerated. This error is then allocated to system contributors. In the case of wavefront error allocation this can be done assuming errors are either statistically independent or directly additive (as is the case with thermally driven power). A typical budgeting activity involves a weighted root-sum-square (RSS) allocation with the most difficult to control error sources being given relatively greater weights in the process. Where directly additive wavefront power terms exist, an additive error term must be included. The overall RSS system wavefront error, E_s, can then be written:

$$E_s = \left(\sum_{i=1}^{n} (W_i\ E_i)^2\right)^{1/2} + \sum_{i=1}^{n} P_i \qquad (1)$$

where W_i are error weights, E_i are the contributor RMS errors (power removed) and P_i are the RMS power levels associated with the n contributors.

A typical error allocation activity can be illustrated in block diagram form as in Figures 1 and 2. Figure 1 shows generic allocation of total system error to three major factors. Figure 2 shows a further allocation of element error to thermal and manufacturing error sources. In many cases, design residuals, alignment defect induced and manufacturability related errors can be reduced to relatively small values, leaving thermally induced errors as the major errors in a system.

A single numerical example to illustrate the error allocation process is appropriate here. For a system requirement of 0.1 waves (RSS) and equal weighting (W_i = 1 for all i),

$$E_r = E_e = E_a = 0.057 \text{ waves RMS} \qquad (2)$$

A simple reflecting system consisting of five elements manufactured to 0.007 waves RMS surface error permits allocation of 0.047 waves RMS to thermally driven errors. This error must account for the thermal response of the system elements, allows only 0.009 waves contribution per element and emphasizes the need to control thermal effects carefully. Next we need to evaluate the effects of moderate thermal loads on optical elements.

Thermal loads on elements

The net thermal load impressed on an element depends on the incident flux density, the surface absorptance, the element area irradiated and the energy loss mechanisms operating for a given thermal-mechanical geometry. A number of element geometries and element mounting approaches are possible. For the simplest case, the element is uniformly irradiated with an absorbed flux of Q/A watts/cm^2 and is in radiation equilibrium with its environment. The equilibrium element temperature T is approximately determined by

$$Q = \sigma A \varepsilon [T^4 - T_\infty^4] \qquad (3)$$

where σ is the Stefan-Boltzman constant, ε is the element surface emissivity and T_∞ is the environment (sink) temperature. Conduction and convection are assumed zero. Figure 3 shows the element temperature predicted for a 270°K sink temperature, ε = 0.8, and for a range of Q/A. The figure shows curves for both the single sided and double sided radiation cases. Where the optical systems involve elements only a few centimeters in diameter (or, more properly, where the thermal load is only a few centimeters in diameter) the predicted element temperatures are too high to give any faith in coating behavior or in acceptable surface figure. Element thermal-mechanical designs must be implemented that will reduce the average temperature while at the same time controlling gradients and thus ensuring acceptable surface figure.

Selection of element configuration

Two types of element-mount geometries can be considered. These are radiatively coupled elements and conductively coupled elements. The simplest configuration, one that most closely corresponds to the thermal case represented by Figure 3, is based on radiation cooling from the element surfaces only. This configuration is shown in Figure 4A. It features a high degree of isolation from the mount to insure minimal higher order surface figure error. Figures 4B, 4C and 4D illustrate several conductive fin configurations. The primary means of cooling for these configurations is also radiation, however, the extension of the radiating area results in lower operating temperature. The effectiveness of the fin in removal of heat from the irradiated area is critical to the resulting element temperature as well as the radial and axial gradients which develop.

The calculated face temperatures for the three fin cases are shown in Figure 5. A 4 cm flux load diameter is assumed. Temperatures are for a nominal 2.5 watts absorbed on the element. While all fins reduce the face temperature, the higher conductivity of the aluminum fins results in a more significant decrease. The relatively low face temperature of the rear coupled geometry (Figure 4D) suggests that a conductive link to a heat sink should also be evaluated. This geometry is illustrated in Figure 6 which shows a mirror

cooled with the aid of a conductive strap. A copper back plate is attached to the mirror with a thin (.25 mm) RTV layer. This plate is conductively coupled by a flexible element to a heat sink, isolated from the optical system, for rejection of heat by any convenient means. The peripheral mount shown is assumed to have negligable conductivity. System geometry requirements are, in part, established by this peripheral mount. They are not dependent on any mechanical elements which are part of the heat flow path. A simple five node closed form thermal model was used to compute the front surface and axial gradient values as a function of Q/A. The front surface temperature and axial gradient are shown for several element thicknesses in Figure 7. Both face temperature and axial gradient can be held to acceptable values. Since axial gradients are moderate and radial gradients are very small due to the copper disk conductivity, bending of the elements is mostly power. This is preferable to the gradients to be expected from the fin geometries. The balance of our considerations will assume a conductive strap cooled element geometry.

System Error Control

The conductively cooled element response needs to be interpreted in light of our overall system wavefront error budgeting and allocation process. Specific numerical error allocations depend upon specific system requirements and system form. It is not the intent of this paper to address any specific system but to consider the issue of system and element thermal response in a general context. The goal then, is to minimize the $E_i P_i$ term in (1) through manipulation of the response of individual elements. This is an acceptable and realistic goal so long as the thermal loading is generally symmetric on each element in a system. For front surface heating and positive material coefficient of thermal expansion (CTE), the radius of curvature and sag changes are:

$$R = R_o \left[1 + 2\alpha\Delta T\right]^{1/2} + t/\alpha\Delta T_{ax} \tag{4}$$

$$SAG = (D_o^2/4R_o)\alpha\Delta T + (D_o\alpha\Delta T)^2/8R \tag{5}$$

where R_o is the initial element vertex radius of curvature, α is the linear CTE, ΔT is the average temperature rise, t is the average element thickness, ΔT_{ax} is the axial (front to back) temperature difference and D is the element diameter. We assume radial gradients to be small compared to ΔT_{ax}.

In Figure 8 we plot estimated mirror sag as a function of Q/A for both ULE and fused silica substrates. These values were then checked using a finite element model of the mirror, RTV, copper disk and conductive strap assuming no mechanical connection through the RTV (modulus of elasticity = 0). The incorporation, in the finite element model, of real material properties for the RTV, leads to revised sag estimates for the two substrates. These values are shown in Figure 8 as dashed lines. Note especially that the predicted deflections for the materials have opposite sign. Finite element predictions are derived from a 62 node thermal model and a 338 node NASTRAN model.

We can see that adjustment of the ULE or fused silica substrate thickness, copper thickness and effective values of Q/A for various elements in a system can provide a substantial reduction in overall system focus shift or residual power. By making use of the opposite sense of deflections with ULE and fused silica mirrors in a multi-element reflective system we can, in cases where steady state operating conditions exist, also provide room temperature factory setting of focus that will be valid, within budget limits, at the operating temperature.

This ability to significantly reduce the thermally driven power or defocus assumes of course, that there are enough elements in the system to make such a balancing possible.

In summary, we have evaluated several forms for reflecting elements in medium power systems and shown that there can exist selections of conductively cooled elements that reduce the net thermally driven power or defocus to a small level and that this approach can be accommodated in system budgeting and in permitting room temperature system setup.

Acknowledgements

The authors would like to thank M. S. Janosky for performing the finite element evaluation of conductively cooled elements and K. A. Havey, Jr., for valuable work in developing portions of the closed form analysis that led to the overall element configuration selection.

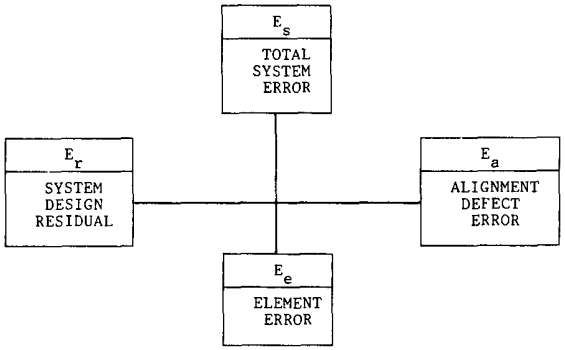

FIGURE 1
SYSTEM RSS ERROR ALLOCATION BROKEN INTO THREE MOST MACROSCOPIC CONTRIBUTORS

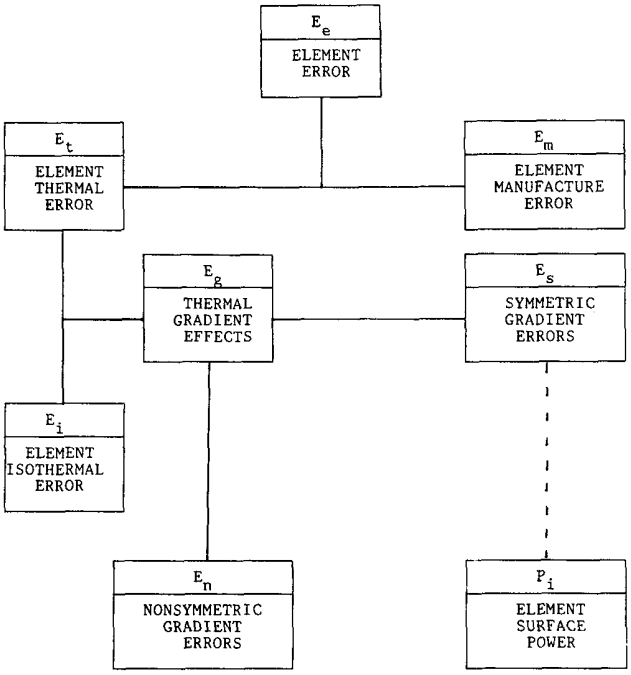

FIGURE 2
RMS ELEMENT ERROR E_e ALLOCATED TO MANUFACTURING AND THERMAL LOAD DRIVEN FACTORS WITH THE THERMAL ERROR CONTRIBUTORS SHOWN

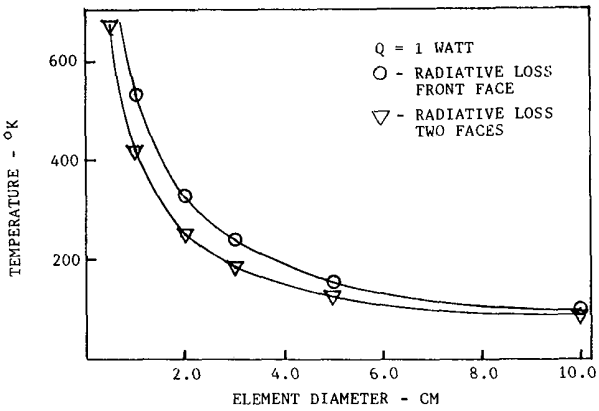

FIGURE 3
ELEMENT FACE TEMPERATURE FOR FULLY IRRADIATED FACE FOR CONSTANT INPUT POWER FOR ONE AND TWO SIDED RADIATION LOSS

FIGURE 4A
RADIATION COOLED ELEMENT WITH THERMALLY ISOLATED MOUNT

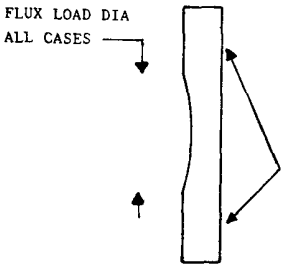

FIGURE 4B
RADIATION COOLED ELEMENT WITH EXTENDED DIAMETER

FIGURE 4C
RADIATION COOLED ELEMENT WITH RADIAL FIN, RADIAL ATTACHMENT

FIGURE 4D
RADIATION COOLED ELEMENT WITH RADIAL FIN, BACK SURFACE ATTACHMENT

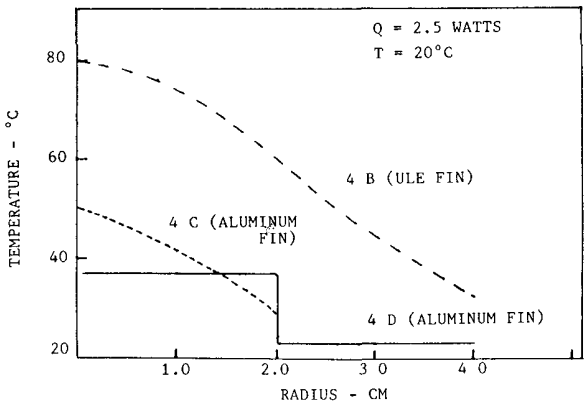

FIGURE 5
ELEMENT FACE TEMPERATURE FOR THREE COOLING FIN CONFIGURATIONS FOR 4CM DIAMETER INPUT

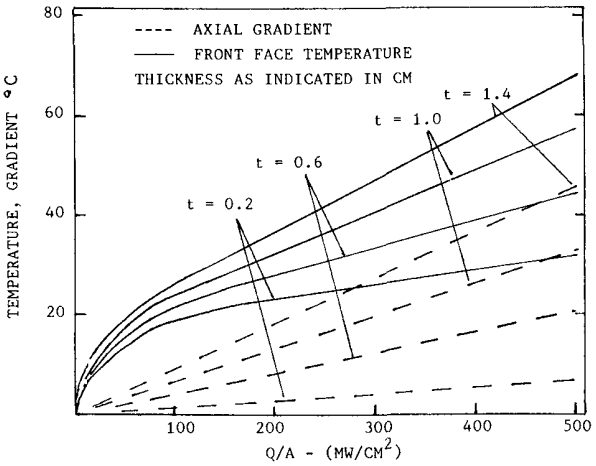

FIGURE 7
FRONT SURFACE TEMPERATURE AND AXIAL GRADIENT vs THICKNESS AND Q/A FOR NOMINAL 2.5 WATTS DEPOSITED

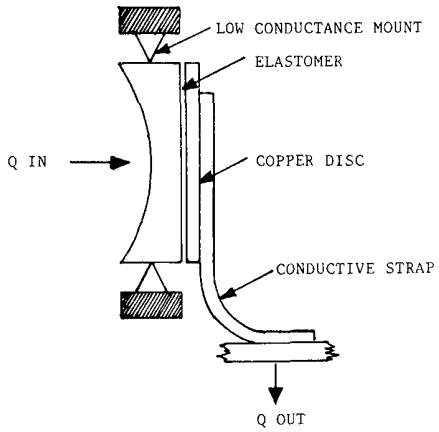

FIGURE 6
CONDUCTIVE STRAP APPLIED TO MIRROR COOLING

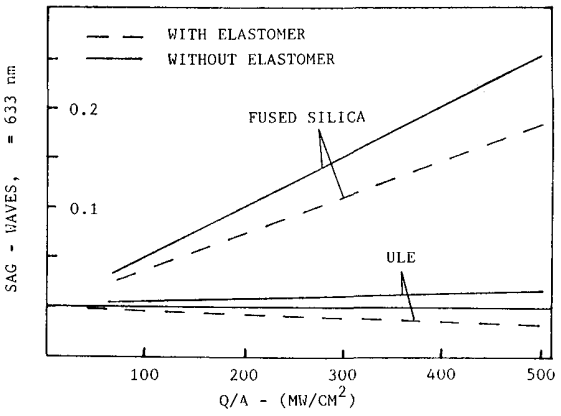

FIGURE 8
SURFACE SAG FOR CONDUCTIVELY COOLED MIRROR AS A FUNCTION OF MIRROR MATERIAL AND FLUX DENSITY FOR Q = 2.5 WATTS, ∋ = 0.8 AND 0.01" THICK ELASTOMER